Emission Phases of Implosion X-Ray Sources for Absorption Spectroscopy

D. A. Chin,[1,2] J. J. Ruby,[1,2] P. M. Nilson,[1] D. T. Bishel,[1,2] F. Coppari,[3] Y. Ping,[3] A. L. Coleman,[3] R S. Craxton,[1] J. R. Rygg,[1,2,4] and G. W. Collins[1,2,4]

[1]Laboratory for Laser Energetics, University of Rochester
[2]Department of Physics and Astronomy, University of Rochester
[3]Lawrence Livermore National Laboratory
[4]Department of Mechanical Engineering, University of Rochester

At LLE's Omega Laser Facility, thin plastic shells were directly driven with ~20 kJ, resulting in a time-integrated x-ray yield of ~10^{12} ph/eV/sr at 7 keV. Using temporally, spatially, and spectrally discriminating diagnostics, three x-ray emission phases were identified: corona emission produced by the laser ablation of the shell, core stagnation, and afterglow emission due to the expanding hot material after stagnation. The newly measured corona and afterglow emission phases account for ~25% of the total x-ray signal and produce x-ray emission at a different time or larger radius than previously considered. The resulting implications of this additional emission for x-ray absorption fine structure (XAFS) spectroscopy are discussed.

This work presents a comprehensive measurement of the temporal, spatial, and spectral x-ray emission of implosion GDP (glow-discharge polymerization) shells on the OMEGA Laser System and identifies three experimental x-ray emission phases consisting of the corona, core stagnation, and afterglow. During the corona phase, the laser illuminates the shell, producing x-ray emission and driving a shock through the shell, causing the material to release inward. When the remaining material reaches the center, it stagnates, reaching Gbar pressures and producing a bright x-ray flash. After stagnating, the remaining material decompresses at Gbar pressures, remaining hot enough to emit x rays for a brief period of time. A schematic of each x-ray emission phase is shown in Fig. 1. To characterize the different emission phases, x-ray emission models were verified using a hydrodynamic simulation and fit to experimental data. The details of each emission phase are shown in Table I.

Table I: Fraction of the total emission in each phase obtained by fitting the streaked spectrum. The fractions are shown along with the 68% credible interval, which was calculated from uncertainty in the fit along with the variability between shots. The time duration was also calculated from the fit and represents the time interval that contains 95% of the signal. Lastly, the diameter was estimated from the time-integrated and time-resolved imaging.

	Corona	Core	Afterglow
Signal fraction	12^{+2}_{-2}	76^{+7}_{-6}	12^{+7}_{-6}
Time duration (ns)	0.2 to 1.1	1.0 to 1.1	1.1 to 1.4
Diameter (μm)	~850	~50	~300

The different spatial profiles of the x-ray sources directly impact the spectral resolution of the XAFS measurement. Using the Rowland (Yaakobi) x-ray spectrometer (XRS) as an example XAFS spectrometer, the impact of these three phases on the XAFS measurements can be estimated. An iron synchrotron absorption spectrum[1] was assumed to be the spectrum for a point source. To simulate the XAFS spectrum for the different source sizes, the point-source absorption spectrum was convolved with a Gaussian

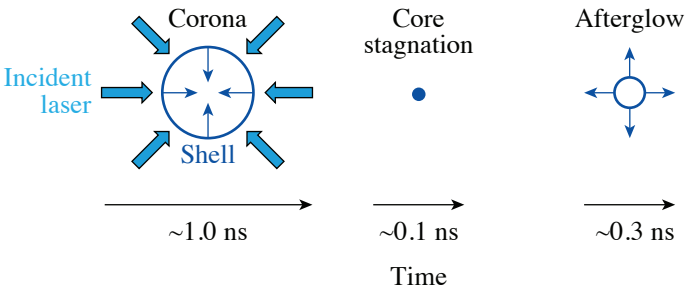

Figure 1
The x-ray emission occurs in three different phases: First, the incident laser causes the shell to emit x rays as the shell is ablated. Second, when the shell material stagnates in the center, there is a bright flash of x-ray emission. Finally, the remaining shell material expands and continues to emit x rays. The estimated time scale corresponds to an 865-μm-outer-diam, 9-μm-thick GDP shell.

function[2] whose full width at half maximum corresponded to the spectral resolution of each emission phase. The total signal was estimated by adding the signals from all three sources in transmission space while including the fractional weights from Table I.

The x-ray absorption near-edge spectroscopy (XANES) spectrum for each of the three phases along with the total signal is shown in Fig. 2(a). While the core spectrum is able to capture the majority of the features of the XANES spectrum, the corona and afterglow phases cannot. This is reflected in the total signal, which is not able to duplicate all of the features in the XANES spectrum. For example, the total spectrum loses the modulation, highlighted with the red arrow (in the inset plot), which can be used to distinguish structural changes and melting in iron.[3] Furthermore, the slope of the total spectrum is decreased, which must be accounted for when extracting the electron temperature.[4] Figure 2(b) shows the degraded extended x-ray absorption fine structure (EXAFS) spectra with each of the three phases and the total spectrum. Temperature can be extracted from the damping in the EXAFS modulations, and, under the harmonic approximation, this damping is given by $e^{-2k^2\mathrm{DWF}}$, where DWF represents the Debye–Waller factor.[5] Fitting[6] the point source and total signal spectra with this harmonic EXAFS approximation, the total signal spectrum has a DWF that is 16±6% larger. It should be noted that other spectrometers will have different spectral resolutions for each emission phase and will be impacted differently. Finally, these spectra represent a sample in a single thermodynamic state for the duration of the backlighter emission. If the material was not in a uniform thermodynamic state, each emission phase could potentially probe the material at a different density, temperature, or crystallographic structure resulting in shifting, amplifying, or decreasing XAFS modulations in unexpected ways.

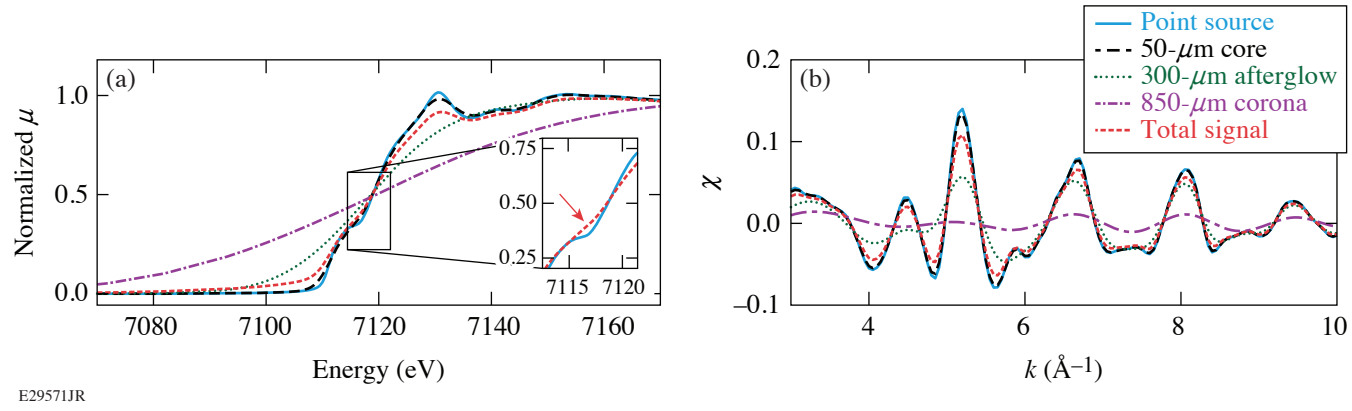

Figure 2
Iron XAFS spectra degraded with the three source sizes, assuming the XRS spectral resolutions. Iron synchrotron data[1] are assumed to give the point-source spectra. (a) XANES spectra as the normalized absorption coefficient (μ). The inset plot compares the point source and total signal with the other lines removed for visibility. The red arrow highlights a modulation that can be used to distinguish structural changes or melting in iron.[3] (b) The EXAFS data as $\chi(k)$ with E_0 = 7118 eV (Ref. 2).

This material is based upon work supported by the Department of Energy National Nuclear Security Administration under Award Number DE-NA0003856, the University of Rochester, and the New York State Energy Research and Development Authority. The support of DOE does not constitute an endorsement by DOE of the views expressed in this paper. D. Chin acknowledges

DOE NNSA SSGF support, which is provided under Cooperative Agreement No. DE-NA0003960. This collaborative work was partially supported under the auspices of the U.S. Department of Energy by Lawrence Livermore National Laboratory under Contract No. DE-AC52-07NA27344.

1. International X-Ray Absorption Society: Fe Data, IXAS X-Ray Absorption Data Library, Accessed 10 May 2021, https://xaslib.xrayabsorption.org/elem/.
2. B. Ravel and M. Newville, J. Synchrotron Rad. **12**, 537 (2005).
3. M. Harmand *et al.*, Phys. Rev. B **92**, 024108 (2015).
4. B. Kettle *et al.*, Phys. Rev. Lett. **123**, 254801 (2019).
5. E. Sevillano, H. Meuth, and J. J. Rehr, Phys. Rev. B **20**, 4908 (1979).
6. B. Ravel and M. Newville, J. Synchrotron Rad. **12**, 537 (2005).